

# Volcanic passive continental margin beneath Maitri station in central DML, East Antarctica: constraints from crustal shear velocity through receiver function modelling

Sandeep Gupta , Nagaraju Kanna  & A. Akilan

Council of Scientific and Industrial Research, National Geophysical Research Institute, Hyderabad, India

## ABSTRACT

Dronning Maud Land (DML) in East Antarctica is considered to be a key area for the reconstruction of the Gondwana supercontinent. We investigate the crustal shear wave velocity ( $V_s$ ) model beneath the Maitri station, situated in the central DML of East Antarctica, through receiver function modelling. The analysis shows an average crustal thickness of  $38.50 \pm 0.5$  km and a  $V_p/V_s$  ratio of  $1.784 \pm 0.002$ . The obtained  $V_s$  structure suggests that the topmost ca. 2.5 km of the crust contains ice and sediments with low  $V_s$  (1.5–2.0 km/s). This layer is underlain by a thick (ca. 12.5 km) layer of  $V_s = 2.25$ –2.6 km/s, suggestive of an extrusive igneous rock (rhyolite) at this depth range. Between 16 and 28 km depth, the  $V_s$  increases from 2.9 to 3.4 km/s. In the lower crust, a 7 km thick layer of  $V_s = 3.9$  km/s is followed by 6 km thick underplated layer ( $V_s = 4.1$  km/s) at the crust–mantle boundary. The uppermost mantle  $V_s$  is ca. 4.3 km/s. With the observation of underplated material in the lowermost crust, extrusive volcanic rocks in the upper crust, seaward dipping reflectors in the surrounding and a general paucity of seismicity, we believe the crust beneath the Maitri station represents a volcanic passive continental margin. We also believe that after its origin in the Precambrian and during its subsequent evolution it might have been affected by the post-Precambrian tectono-thermal event(s) responsible for the Gondwana supercontinent break-up.

## KEYWORDS

Crustal shear velocity; volcanic passive margin; Maitri station; Dronning Maud Land; underplated lower crust; neighbourhood algorithm

## ABBREVIATIONS

CSIR-NGRI: Council of Scientific and Industrial Research – National Geophysical Research Institute; DML: Dronning Maud Land; RF: receiver function

## Introduction

The Antarctic plate has a unique tectonic setting. It is surrounded almost completely by divergent margins, with a very small amount of convergent or transformed margins. The Antarctic continent is roughly divided into two large tectonic provinces: East Antarctica and West Antarctica, divided by the Transantarctic Mountains (Fig. 1a). West Antarctica is a chain of many islands beneath the ice sheet of the Cenozoic Era attributed to active volcanoes (Kaminuma 2006). East Antarctica is considered as a stable, cratonic block with a Precambrian basement. Limited geological samples are available from this region covered by thick ice, but several geophysical studies have revealed the average crustal and upper mantle structure in East Antarctica to define its geo-tectonics. The average crustal thickness in East Antarctica is reported to be ca. 40 km (e.g., Malaimani et al. 2008; Bayer et al. 2009; Baranov & Morelli 2013). With a ca. 20 km thick upper crust and a slightly higher-than-normal seismic velocity, Bentley (1983) reported a typical continental crust for East Antarctica. Surface wave studies found craton-like velocities

in East Antarctica (Bentley 1991; Ritzwoller et al. 2001). A deep electrical conductivity structure under Schirmacher Oasis in central DML showed highly resistive (8000–10 000 ohm m) upper crust followed by lesser resistive (500–600 ohm m) lower crust; and the results were interpreted that the Schirmacher Oasis to be a stable cratonic platform (Murthy et al. 2013). Another magnetotelluric study in the Schirmacher Oasis (Fig. 1) revealed that the crust had a higher resistive (103 to ca. 104 ohm m) upper layer underlain by a moderately resistive (100–300 ohm m) layer and the Moho was at 32–38 km (Abdul Azeez et al. 2015). A regional gravity study showed that the Moho depth was ca. 32 km below the Schirmacher Oasis (Verma et al. 1994). The heat flow in much of East Antarctica was reported to be ca. 50 mW m<sup>-2</sup> or more (Siegert 2000) and the observed thermal anomalies were related to the mantle plume (Hole & Lemasurier 1994). The Magnetotelluric data (Ritzwoller & Bentley 1983) showed that the regional negative magnetic anomaly in central DML could be indicative of an intensive thermal reactivation of DML due to late Precambrian tectono-thermal activity, which might have caused an up-doming of the Curie isotherm

**CONTACT** Sandeep Gupta  [sandeepgupta@ngri.res.in](mailto:sandeepgupta@ngri.res.in)  Council of Scientific and Industrial Research, National Geophysical Research Institute, Uppal Road, Hyderabad 500007, India

 The supplementary material for this article can be accessed [here](#).

© 2017 The Author(s). Published by Informa UK Limited, trading as Taylor & Francis Group.

This is an Open Access article distributed under the terms of the Creative Commons Attribution-NonCommercial License (<http://creativecommons.org/licenses/by-nc/4.0/>), which permits unrestricted non-commercial use, distribution, and reproduction in any medium, provided the original work is properly cited.

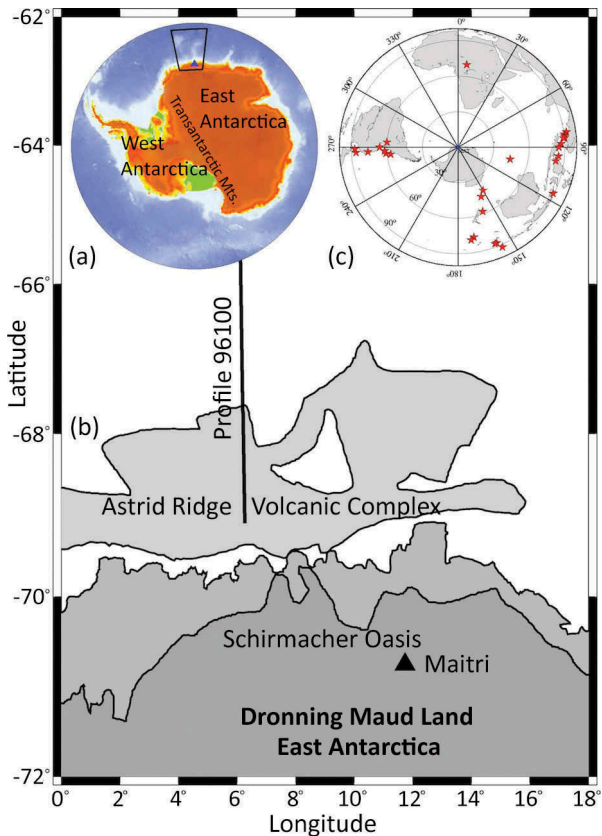


**Figure 1.** (a) Topography map of Antarctica showing the study region (trapezoid-shaped box) and the major tectonic units: East Antarctica, West Antarctica and the Transantarctic Mountains. (b) Simplified tectonic map of the study region (after Jokat et al. 2004). The triangle represents the Maitri seismic station. (c) Epicentre distributions of 29 teleseismic earthquakes (red stars) used to calculate RFs.

and might thus have reduced the thickness of the magnetically active crust (Bormann et al. 1986). The Antarctic Digital Magnetic Anomaly Project compilation provided important constraints on the break-up processes and igneous activity related to the formation of the passive margin of East Antarctica (Golynsky et al. 2013). East Antarctica has not experienced any significant tectonic deformation and its lithosphere may still be preserving the crustal and upper mantle characteristics inherited during the evolution of the Gondwana supercontinent. Moreover, DML is composed of different crustal blocks of varying ages from Archean to early Paleozoic and is considered to be a key area for the reconstruction of the Gondwana supercontinent, containing continental fragments of both East and West Gondwana (Riedel et al. 2013; Mieth & Jokat 2014). Using limited direct geological sampling and the average crust–upper mantle structure from geophysical studies of this critically located region, various tectonic models were proposed for the history and geometry of the Gondwana supercontinent break-up (e.g., Mieth &

Jokat 2014 and references therein). A detailed study of the crustal structure and the nature of intra-crustal layers can be very useful for understanding the mechanism responsible for the breakup of the Gondwana supercontinent and also the dynamics of plate motions. Therefore, in this study we investigated in detail the crustal shear wave velocity ( $V_s$ ) structure beneath the Maitri broadband seismic station ( $70.76^\circ\text{S}$ ;  $11.73^\circ\text{E}$ ) in East Antarctica through modelling of teleseismic RF and studied the possible role of this region in the Gondwana geodynamics.

The Maitri broadband seismic station is in the Indian Antarctica base station located in Schirmacher Oasis, near the Princess Astrid Coast, East Antarctica (Fig. 1b). Schirmacher Oasis is a coastal nunatak in the central DML. The exposed rocks in central DML indicate that it is probably related to a major tectono-thermal event at ca. 650–490 Mya—the Pan-African event (Mieth & Jokat 2014). A sequence of seaward dipping reflectors, associated with middle to late Jurassic volcanism was reported off central DML (Hinze & Krause 1982). Jacobs et al. (2003) proposed an asthenospheric upwelling, followed by the mantle delamination of the orogenic root for the central DML.

## Data

We used data recorded by a permanent broadband seismic station at Maitri during 2006–08, operated by the CSIR-NGRI (Fig. 1b). The station configuration includes a CMG 3ESP sensor with a flat velocity response between 100 s and 50 Hz and a Reftek 72A 121–03 data logger. Data was continuously recorded at 50 samples/s and GPS time was logged.

We computed RFs using the iterative time domain deconvolution approach (Ligorria & Ammon 1999) from good signal-to-noise ratio earthquakes of magnitude ( $m_b$ )  $> 5.5$  in the epicentral distance  $30$ – $95^\circ$  (Fig. 1c). To minimize the influence of the coastal noise on the RFs, a two-pole high pass filter with a corner frequency of 0.02 Hz was applied to the waveforms. RFs were calculated using Gaussian width corresponding to low pass filters with corner frequencies of 2.4, 1.25, 0.7, 0.5 Hz. For further analysis, we used only the RFs with variance reduction cut-off above 80% and the direct  $P$ -wave within one second of the zero time on the deconvolved trace. At higher frequencies, the RFs were noisy while at lower frequency these were smoothed out. As we aimed at mapping the crust–mantle boundary along with other intra-crustal layers, we preferred to use the RF with Gaussian width 1.6 for further analysis. All the calculated RFs with respect to back-azimuth (left axis) and epicentral distance (right axis) are presented in Supplementary

Fig. S1. The Moho converted  $P$ -to- $S$  ( $P_s$ ) phase was observed at ca. 5 s with its multiples at ca. 16 s and ca. 21 s.

### Receiver function modelling

In order to minimize the effects of noise and aid in visually enhancing coherent arrival, RFs with good signal-to-noise ratio were stacked in a narrow epicentral distance and back-azimuth bins. Figure 2a shows the six individual RFs for back-azimuth 83–95° and epicentre distance 85–90°, which were stacked (Fig. 2a) for further analysis and determination of the velocity structure beneath the study region.

### Moho depth and $V_p/V_s$ ratio estimation

To obtain the Moho depth ( $H$ ) and average  $V_p/V_s$  ratio, we used the  $H$ - $V_p/V_s$  stacking technique of Zhu and Kanamori (2000), which is a well-established technique and exploits the fact that the arrival times of the specific Moho converted phase and multiples appearing on RFs are determined by known functions of Moho depth ( $H$ ),  $V_p/V_s$  ratio and average crustal  $P$ -wave velocity ( $V_p$ ). We used an average  $V_p$  of 6.25 km/s.  $H$  and  $V_p/V_s$  ratio were allowed to vary from 20 to 50 km (with 0.05 km increment) and 1.6–

1.9 (with 0.002 increment), respectively. In the computation, based on amplitudes of  $P_s$ ,  $PpPms$  and  $PpSms+PsPms$  phases, we assigned different weights of 0.6, 0.3 and 0.1, respectively. We followed the same procedure with  $V_p$  variations at  $\pm 0.1$  km/s to constrain  $H$  and  $V_p/V_s$  ratios. Figure 2b shows the result from the  $H$ - $V_p/V_s$  grid search technique and the result is discussed later.

### Shear wave velocity mapping

We mapped the  $V_s$  variation with depth beneath the Maitri seismic station from the stacked RF (Fig. 2a) following the nonlinear neighbourhood algorithm proposed by Sambridge (1999) and as in Gupta et al. (2010). The method assumes a one-dimensional isotropic velocity model. It is a multi-dimensional parameter space search algorithm that only needs to solve the forward problem and does not require the computing of partial derivatives of the RFs. This method uses an ensemble-based Monte Carlo search technique to find the set of velocity models which best satisfy the objective function. We used, as our objective function, a scaled L2-norm of the difference between the theoretical and the observed RF.

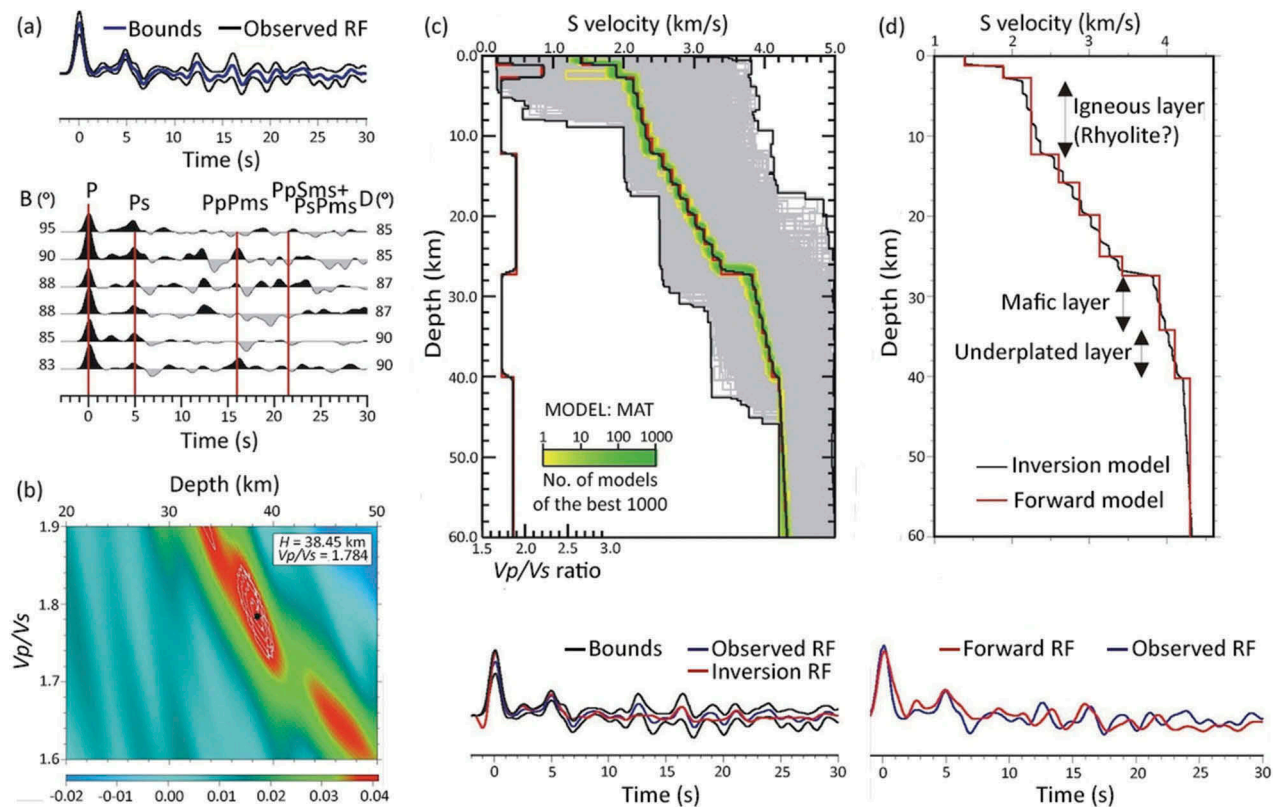


**Figure 2.** (a) Plot showing the stacked RFs used to infer the crustal structure beneath the Maitri station. Below this are the six RFs used for stacking. (b) Plot showing the results of the  $H$ - $V_p/V_s$  stacking technique (Zhu & Kanamori 2000) for the stacked RFs shown in (a). The black dot within the contour represents the maximum amplitude; the corresponding  $H$  and  $V_p/V_s$  values are shown in the rectangular box. (c) One-dimensional shear velocity models obtained from the neighbourhood algorithm inversion (Sambridge 1999). Details are given in the text. (d) Simplified shear velocity model (red line) along with different layers, shown along with the final inversion model (black line). Details are given in the text.

In this study, we used a time-window of 30 s and a 24-dimensional parameter space, defined by six flat layers, each with four parameters (layer thickness,  $V_s$  at the top and bottom of each layer, and  $V_p/V_s$  ratio). The two  $V_s$  parameters in each layer allow the definition of a velocity gradient for that layer, which allows the representation of a large number of potential velocity–depth distributions. Very loose a priori constraints were placed on the minimum  $V_s$  and maximum  $V_s$ , the layer thicknesses, as well as  $V_p/V_s$ . The model parameterization is shown in Supplementary Table S1. Each inversion run involved 200 iterations, generating 20 100 velocity models. The stability of the inversion solutions was tested using a large range of initial random seeds, incidence angles, and velocity model parameterizations. In Fig. 2c, the best fit  $V_s$  model (solid black line) along with all other models (solid grey lines) that fit the RFs are also displayed. The green region depicts the best 1000 velocity models and the red solid line represents an average of these 1000 models. The  $V_p/V_s$  ratio variation for the best model (black line) and for an average model (red line) is shown in the left side of Fig. 2c. The one-dimensional velocity model obtained by the inversion process is able to model the dominant phases in the RF. The calculated RF (red line) and the observed stacked RF (blue line) with  $\pm 1\sigma$  bounds (black lines) are shown in the bottom of Fig. 2c. Figure 2d shows the simplified model (red line) of the final model (black line) from inversion and matching of the calculated RF (red line). The observed RF is shown in the bottom of Fig. 2d. Figure S2 shows the corresponding Moho piercing point and the back-azimuth direction which were imaged by this velocity model.

## Results and discussion

Beneath Maitri station, the Moho depth is  $38.50 \pm 0.5$  km and the average  $V_p/V_s$  is  $1.784 \pm 0.002$  (Fig. 2b). The Moho depth is in agreement with earlier estimates for this region, using RF analysis (Malaimani et al. 2008), RF analysis and modelling of a seismic refraction profile (Bayer et al. 2009), and a compilation of various available data from seismic reflection/refraction and RFs (Baranov & Morelli 2013). The higher  $V_p/V_s$  ratio suggests an intermediate-to-mafic crust beneath this region. The  $V_s$  model (red colour line in Fig. 2d) indicates that the top ca. 1.0 km thick layer of ice with low  $V_s$  (ca. 1.4 km/s) is underlain by a thin (ca. 1.5 km) layer of sediments ( $V_s$  ca. 1.9–2.0 km/s). These layers are underlain by a ca. 12.5 km thick layer of  $V_s = 2.25$ –2.6 km/s. In this depth range, equivalent to ca. 300–400 MPa pressure, a layer with  $V_s = 2.25$ –2.6 km/s can be indicative of rhyolite (an extrusive igneous) rock (Christensen & Stanley 2003). At a depth of 16–28 km we observe that  $V_s$  increases from

2.9 to 3.4 km/s. At a depth of 28 km, we find a ca. 7 km thick layer of  $V_s = 3.9$  km/s, representing lower crustal mafic material. This layer is followed by a 6 km layer of  $V_s = 4.1$  km/s and another layer of  $V_s = 4.3$  km/s below. We believe that the layer with  $V_s = 4.3$  km/s represents the upper mantle, as reported by earlier studies (e.g., Ritzwoller et al. 2001; Bayer et al. 2009). It is interesting to observe a transitional layer ( $V_s = 4.1$  km/s) between lower crust ( $V_s = 3.9$  km/s) and the uppermost mantle ( $V_s = 4.3$  km/s). Similar observations have also been reported from many continental margins in the world (e.g., Thybo & Artemieva 2013 and references therein). Therefore, we think that this layer is evidence of underplated material in the lowermost crust and points to the presence of a continental margin beneath the study region. The apatite-fission-track data and the high-elevation margin morphology study of central DML also suggest a typical passive nature for this region (Meier 1999).

By combining our result with available knowledge from this region (the presence of underplated material in the lowermost crust, extrusive rocks (rhyolite) in the upper crust, seaward dipping reflectors (Hinz & Krause 1982) and a lack of seismicity (Kaminuma 2006), we suggest that the crustal structure below the Maitri station in the Schirmacher Oasis represents a volcanic passive continental margin rather than a typical continental crust. This view also gets support from the crustal seismic velocity structure along seismic refraction profile 96100 (to the north-west of our study region; Fig. 1b), reporting this region as a volcanic continental margin (Jokat et al. 2004), as well as many other studies (e.g., Geoffroy 2005, and references therein).

Further, regarding the possible mechanism responsible for the obtained crustal structure beneath central DML we speculate that the crust in this region was probably formed during the Precambrian. During its evolution with time it was affected by post-Precambrian tectono-thermal event(s) (e.g., the Pan-African) and/or by the Karoo–Maud plume. The latter also affected southern Africa and the western part of East Antarctica through its penetration into the upper lithosphere at about 180 Mya and is considered to be one of the main factors for the break-up of Gondwana supercontinent (Sushchevskaya et al. 2009).

## Conclusion

To study the role of DML, East Antarctica in the reconstruction of the Gondwana supercontinent, we investigated the crustal  $V_s$  structure beneath the Maitri seismic station situated in the Schirmacher Oasis, central DML. Through analysis and modelling of the teleseismic RFs calculated at the seismic station, the  $V_s$  structure suggests

that the uppermost 2.5 km consist of ice and sediments ( $V_s = 1.5\text{--}2.0$  km/s) and are underlain by 12.5 km of extrusive igneous rock (rhyolite,  $V_s = 2.25\text{--}2.6$  km/s). Between 16 and 28 km depth,  $V_s$  gradually increases from 2.9 to 3.4 km/s. In the lower crust, a ca. 7 km thick layer of  $V_s = 3.9$  km/s is followed by 6 km thick underplated layer ( $V_s = 4.1$  km/s) at the crust–mantle boundary. The Moho is at ca. 40 km and the uppermost mantle  $V_s$  is ca. 4.3 km/s. The presence of underplated material in the lowermost crust, extrusive volcanic rocks (Rhyolite) in the upper crust, seaward dipping reflectors in the surrounding area and the general paucity of seismicity suggest that the crust beneath the Maitri station is a volcanic passive continental margin and not a typical cratonic continental crust. Combining our results with other studies in this region, we also believe that after its formation in the Precambrian and during its subsequent evolution, it was affected by the post-Precambrian tectono-thermal event(s) responsible for the break-up of the Gondwana supercontinent.

## Acknowledgements

The data used in this study are part of project ILP-0301-28 (VKG/JCK). We thank Prof. M. Sambridge for providing neighbourhood algorithm inversion code used in this study. SG acknowledges support from CSIR-NGRI projects MLP-6505-28 (SKG) and INDEX. The manuscript has been benefited immensely from the constructive comments by two anonymous reviewers and section editor Robert Spielhagen.

## Disclosure statement

No potential conflict of interest was reported by the authors.

## ORCID

Sandeep Gupta  <http://orcid.org/0000-0002-9961-9844>  
Nagaraju Kanna  <http://orcid.org/0000-0002-9919-0574>

## References

- Abdul Azeez K.K., Prabhakar E Rao S., Gupta A.K., Basava S. & Harinarayana T. 2015. Magnetotelluric study across the Schirmacher Oasis of central Dronning Maud Land, East Antarctica: electrical characteristics of the East African–Antarctic Orogen as a possible aid to link Gondwana fragments. Paper presented at the XII International Symposium on Antarctic Earth Sciences, 13–17 July, Goa, India.
- Baranov A. & Morelli A. 2013. The Moho depth map of the Antarctica region. *Tectonophysics* 609, 299–313.
- Bayer B., Geissler W.H., Eckstaller A. & Jokat W. 2009. Seismic imaging of the crust beneath Dronning Maud Land, East Antarctica. *Geophysical Journal International* 178, 860–876.
- Bentley C. 1983. Crustal structure of Antarctica from geophysical evidence—a review. In R.L. Oliver et al. (eds.): *Antarctic earth sciences*. Pp. 491–497. Canberra: Australian Academy of Science.
- Bentley C.R. 1991. Configuration and structure of the sub-glacial crust. In R.J. Tingey (ed.): *The geology of Antarctica*. Pp. 335–364. Oxford: Oxford Science Publications.
- Bormann P., Bankwitz P., Bankwitz E., Damm V., Hurtig E., Kämpf H., Menning M., Paech H.-J., Schäfer U. & Stackebrandt W. 1986. Structure and development of the passive continental margin across the Princess Astrid Coast, East Antarctica. *Journal of Geodynamics* 6, 347–373.
- Christensen N.I. & Stanley D. 2003. Seismic velocities and densities of rocks. In W. Lee et al. (eds.): *International handbook of earthquake and engineering seismology*. Pp. 1587–1594. Amsterdam: Academic Press.
- Geoffroy L. 2005. Volcanic passive margins. *Comptes Rendus Geoscience* 337, 1395–1408.
- Golynsky A.V., Ivanov S.V., Kazankov A.J., Jokat W., Masolov V.N., von Frese R.R.B. & the ADMAP Working Group. 2013. New continental margin magnetic anomalies of East Antarctica. *Tectonophysics* 585, 172–184.
- Gupta S., Mishra S. & Rai S.S. 2010. Magmatic underplating of crust beneath the Laccadive Island, NW Indian Ocean. *Geophysical Journal International* 183, 536–542.
- Hinz K. & Krause W. 1982. The continental margin of Queen Maud Land/Antarctica: seismic sequences, structural elements and geological development. *Geologische Jahrbuch E23*, 17–41.
- Hole M.J. & Lemasurier W.E. 1994. Tectonic controls on the geochemical composition of Cenozoic, mafic alkaline volcanic rocks from West Antarctica. *Contributions to Mineralogy and Petrology* 117, 187–202.
- Jacobs J., Bauer W. & Fanning C.M. 2003. Late Neoproterozoic/early Palaeozoic events in central Dronning Maud Land and significance for the southern extension of the East African Orogen into East Antarctica. *Precambrian Research* 126, 27–53.
- Jokat W., Ritzmann O., Reichert C. & Hinz K. 2004. Deep crustal structure of the continental margin off the Explora Escarpment and in the Lazarev Sea, East Antarctica. *Marine Geophysical Researches* 25, 283–304.
- Kaminuma K. 2006. Seismicity in the Antarctic and surrounding ocean. *Journal of Indian Geophysical Union* 10, 15–24.
- Ligorria J.P. & Ammon C.J. 1999. Iterative deconvolution and receiver function estimation. *Bulletin of Seismological Society of America* 89, 1395–1400.
- Malaimani E.C., Ravi Kumar N., Padhy S., Rao S.V.R.R., Chander G.B., Srinivas G.S. & Akilan A. 2008. Continuous monitoring of seismicity by Indian permanent seismological observatory at Maitri. *Indian Journal of Marine Sciences* 37, 396–403.
- Meier S. 1999. *Paleozoic and Mesozoic tectono-thermal history of central Dronning Maud Land, East Antarctica – Evidence from fission track thermochronology*. *Berichte zur Polarforschung* 337. Bremerhaven: Alfred Wegener Institute.
- Mieth M. & Jokat W. 2014. New aeromagnetic view of the geological fabric of southern Dronning Maud Land and Coats Land, East Antarctica. *Gondwana Research* 25, 358–367.
- Murthy D.N., Veeraswamy K., Harinarayana T., Singh U.K. & Santosh M. 2013. Electrical structure beneath Schirmacher Oasis, East Antarctica: a magnetotelluric study. *Polar Research* 32, 17309.

- Riedel S., Jacobs J. & Jokat W. 2013. Interpretation of new regional aeromagnetic data over Dronning Maud Land (East Antarctica). *Tectonophysics* 585, 161–171.
- Ritzwoller M.H. & Bentley C.R. 1983. Magnetic anomalies over Antarctica measured from MAGSAT. In R.L. Oliver et al. (eds.): *Antarctic earth sciences*. Pp. 504–507. Canberra: Australian Academy of Science.
- Ritzwoller M.H., Shapiro N.M., Anatoli L., Levshin A.L., Garrett M. & Leahy G.M. 2001. Crustal and upper mantle structure beneath Antarctica and surrounding oceans. *Journal of Geophysical Research – Solid Earth* 106, 30645–30670.
- Sambridge M. 1999. Geophysical inversion with a neighbourhood algorithm-I searching a parameter space. *Geophysical Journal International* 138, 479–494.
- Siegert M.J. 2000. Antarctic subglacial lakes. *Earth-Science Reviews* 50, 29–50.
- Sushchevskaya N.M., Belyatsky B.V., Leichenkov G.L. & Laiba A.A. 2009. Evolution of the Karoo–Maud mantle plume in Antarctica and its influence on the magmatism of the early stages of Indian Ocean opening. *Geochemistry International* 47, 1–17.
- Thybo H. & Artemieva I.M. 2013. Moho and magmatic underplating in continental lithosphere. *Tectonophysics* 609, 605–619.
- Verma S.K., Vyaghreswara Rao M.B.S. & Gopal B.V. 1994. Gravity survey (helicopter supported) between Schirmacher Oasis and Wohlthat Mountains, Dronning Maud Land, Antarctica. In: *Ninth Indian Expedition to Antarctica, Scientific Report, 1994. Technical Publication* 6. Pp. 209–217. New Delhi: Department of Ocean Development.
- Zhu L. & Kanamori H. 2000. Moho depth variation in southern California from teleseismic receiver functions. *Journal of Geophysical Research – Solid Earth* 105, 2969–2980.